Journal of Biological Physics **28:** 95–113, 2002.

On the Charge and Molecule Based Summations of Solvent Electrostatic Potentials and the Validity of Electrostatic Linear Response in Water

C. SATHEESAN BABU[1], P.-K. YANG[2] and C. LIM[1,3]
[1] *Institute of Biomedical Sciences, Academia Sinica, Taipei 11529, Taiwan R 0.C*
[2] *Institute of Molecular Medicine, College of Medicine, National Taiwan University, Taipei, Taiwan R.0.C.*
[3] *Department of Chemistry, National Tsing Hua University, Hsinchu 300, Taiwan*

Abstract. Solvent-induced electrostatic potentials and field components at the solute sites of model Na^{+q}–Cs^{-q} molecules were computed by summing over *either* solvent charges (q-summation) or solvent molecular centers (M-summation) from molecular dynamics simulations. These were compared with values obtained by solving Poisson equation with the dielectric boundary defined by $R_{eff} = (R_{atom} + R_{gmax})/2$. q-summation using cut-offs that are $\leq$ 10 Å generally underestimates or overestimates (a) the potentials and field components at Na^{+q} and Cs^{-q} relative to the theoretical values and (b) electrostatic solvation free energies of the dipolar solutes assuming linear solvent response relative to the respective values from free energy simulations. Furthermore, the q-summed electric potentials showed significant oscillations even beyond the second hydration shell. In contrast, the corresponding M-summed potentials plateaued after the first hydration shell. Although the different water molecular centers yielded different converged potential values, the dipole center produced values in remarkable agreement with the theoretical values for solute charges ranging from 1 to 0.1e, indicating the existence of a convenient molecular center for computing these quantities. In contrast to the M-summed *potentials*, the electrostatic field components and electrostatic solvation free energies from linear response relationships were found *not* to be sensitive to the choice of the molecular center for typical cut-off distances (8 to 12 Å) used in most simulations.

Key words: continuum dielectic theory, electrostatic potentials, linear response, M-summation, Poisson equation, q-summation

1. Introduction

Accurate values of solvent-induced electrostatic potentials and electric fields at solute sites are required in molecular theories of polar solvation [1–4], in analyzing redox properties of solutes [5] and in problems related to binding free energy calculations using linear response relationships [3, 6–8]. For a molecular solvent, these quantities can be computed either by summing over charges (q-summation), or by treating the solvent molecule as a group with a chosen molecular (M) center and summing over these M-centers (M-summation) [3, 9–11]. Figure 1 shows the

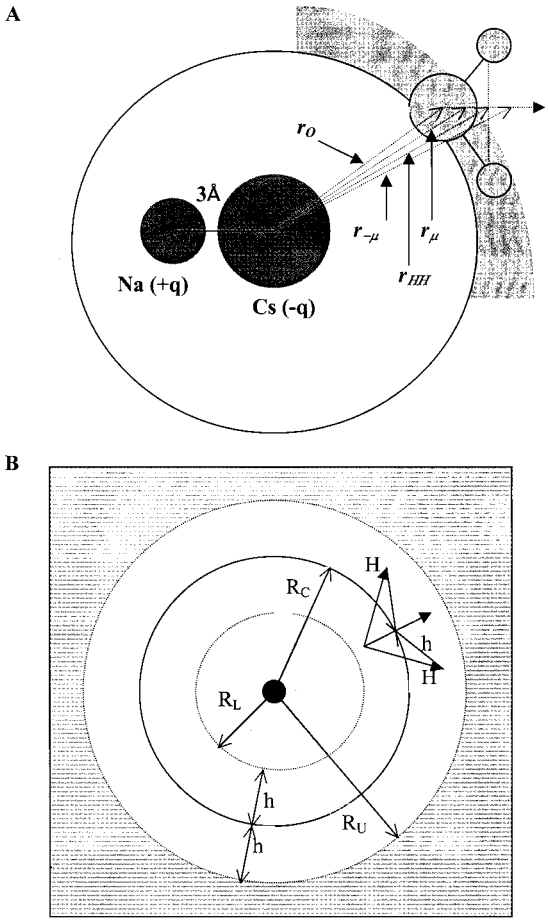

Figure 1. (A) A schematic diagram showing the different water molecular centers, which are used in summing the solvent-induced electrostatic potentials at Cs of the Na^{+q}–Cs^{-q} molecule. r_O, r_μ, r_{HH}, and $r_{-\mu}$ is the distance from Cs to M_O, M_μ, M_{HH} and $M_{-\mu}$, respectively (see Introduction for definitions of the M-centers). For clarity, the geometric center (M_G) is not shown since it is close (within 0.1 Å) to M_O. (B) The three distinct solvent regions around a solute if a spherical cut-off R_C, based on a molecular center of water, is used for the potential calculation. Both q- and M-summed potentials (Equations 1 and 2) are equal inside $R_L = R_C - h$ and beyond $R_U = R_C + h$. The difference between the two summation schemes arises for the unshaded region between R_L and R_U.

geometry of the problem for a model Na^{+q}–Cs^{-q} molecule in a 3-site model of

liquid water. In q-summation, the electrostatic potential due to solvent molecules within a radial distance R from the solute site α, $\phi_\alpha^q(R)$, is computed from [12]:

$$\phi_\alpha^q(R) = 4\pi \sum_X \rho_X \int_0^R \frac{q_X}{r_{\alpha X}} g_{\alpha-X}(r) r^2 dr \tag{1}$$

In Equation 1, X is the water oxygen or hydrogen, $g_{\alpha-X}$ is the solute α-solvent X radial distribution function (rdf), q_X is the charge on X, $r_{\alpha X}$ is the distance between site α and the X atom of the water molecule, and ρ_X is the density of X. In M-summation, $\phi_\alpha^M(R)$ is computed from [11, 13]:

$$\phi_\alpha^M(R) = \int_0^R dr \left\langle \sum_{i=1}^N \delta(r - r_{i,M}) \sum_X \frac{q_X}{r_{\alpha X}} \right\rangle. \tag{2}$$

In Equation 2, N is the number of water molecules, $r_{i,M}$ is the distance of the i^{th} water M-center to the solute site, and the angular brackets denote an ensemble average. A spherical cut-off based on a molecular center divides the solvent into three distinct regions, as illustrated in Figure 1B where the dipole center of water is chosen as the M-center, h is the distance between the center and a water hydrogen, and R_C is the cut-off radius. Equations 1 and 2 yield the same potentials inside $R_L = R_C - h$ as well as outside $R_U = R_C + h$ where $\phi_\alpha^q = \phi_\alpha^M = 0$. The difference between the two schemes arises in the region between R_L and R_U (unshaded region in Figure 1B) since q-summation splits the water charges while M-summation considers the entire molecule so that different net charges are involved in the two summation schemes.

There have been various arguments for and against the use of q- and M-summation. Arguments against the use of M-summation are based on the following findings: (1) The M-summed electrostatic potential at a given solute site depends on the choice of the M-center even when the solute is uncharged [11, 14]. For example, the M-summed electrostatic potential at the center of an *uncharged* SPC water oxygen in SPC water is –9 to –10 kcal mol^{-1} e^{-1} if the M-center is the water oxygen, and –3 kcal mol^{-1} e^{-1} if the M-center is the dipole center [3, 10]. (2) These M-summed values differ from the respective potential computed using Ewald summation with conducting boundary conditions (+10 kcal mol^{-1} e^{-1}), whereas q-summation yields the same value of +10 kcal mol^{-1} e^{-1} [11]. (3) Furthermore, q-summation produces potentials similar to those computed using Gauss' law assuming spherical symmetry of water clusters [15]. (4) M-summation does not yield the expected zero potential at an *uncharged* solute in an ideal gas of water molecules but q-summation does [16].

However, there are just as many arguments against the use of q-summation, in support of the use of M-summation: (1) M-summation avoids splitting of molecular partial charges, which can create a net charge within the cutoff sphere,

causing the potential to oscillate with distance from a solute site [11, 13, 17]. (2) M-summation does not violate intramolecular site-site correlation, whereas q-summation does as the water oxygen and hydrogen atoms are treated as independent particles [13, 18]. Consequently, summation leads to an artifactual induced surface dipole density at the cutoff boundary. (3) M-summation has been shown to yield correct potentials with an appropriate M-center [13, 14, 18]. Åqvist and Hansson [13] as well as Ashbaugh *et al.* [14] equated this unique M-center to the position that yields zero potential on an *uncharged* solute in SPC water at the surface layer around the cut-off. However Åqvist and Hansson found the optimal M-center to be the dipolar center of the water molecule, while Ashbaugh *et al.* found it to lie 0.866 Å away from the water oxygen in the dipole direction (see Figure 1). On the other hand, Vorobjev and Hermans [18] equated the optimal M-center to the position that yields zero potential in the rotational high temperature limit. This position was attributed to the water oxygen for the SPC, TIP3P and TIP4P water models.

Here the electric potentials, field components, and electrostatic solvation free energies from simulations of *polar* solutes (as opposed to uncharged solutes in previous works) are compared with those derived by solving Poisson equation with the dielectric boundary defined by the effective atomic radius (R_{eff}) [19]:

$$R_{eff} = (R_{atom} + R_{gmax})/2 \tag{3}$$

In Equation 3 R_{atom} is the atomic radius of the solute (see below), and R_{gmax} is the first peak-position of the atom-oxygen or atom-hydrogen rdf in liquid water. With the dielectric boundary defined by R_{eff}, Poisson equation can be solved by finite difference methods for the electric potentials, field components, and hence electrostatic solvation free energies. The R_{eff} reflects the specific solute-solvent structure consistent with the thermodynamic state: it depends on the charge of the solute atoms as well as the molecular nature of the solvent. In our previous works, we showed that R_{eff} incorporates the thermodynamic state dependence and molecular nature of the solvent as it could yield accurate hydration free energies, enthalpies and thus entropies of spherical ions [19] as well as solvation free energies of spherical ions in non-aqueous solvents such as dimethyl sulfoxide, acetonitrile and ethanol [20]. Moreover, R_{eff} could reproduce the electrostatic solvation free energies of *non*-spherical solutes derived from free energy simulations in the presence of explicit water molecules [21]. It could also take into account the nonlinear solvent responses around the solute [22].

We chose to study a Lennard-Jones Na^{+q}–Cs^{-q} solute (q = 0.1, 0.3, 0.5, 0.7 and 1.0e) with an internuclear distance of 3 Å in TIP3P [23] water for two reasons. First, systematic errors in the electrostatic potentials and field components due to truncation of long-range Coulombic forces are minimized for a neutral molecule. Second, the van der Waals (vdW) parameters for fully charged Na^+ and Cs^-, which have been calibrated to reproduce the experimental hydration free energies and ion-water distances of the isolated Na^+ and Cs^+ ions [19, 24] are assigned

to the constituent atoms, Na^{+q} and Cs^{-q}, respectively, of the diatomic molecule. Such a choice removes ambiguity in the atomic radius, R_{atom} in Equation 3 for continuum theory calculations since the Pauling ionic radii of Na^+ (0.95 Å) and Cs^- (1.65 Å) can be used for R_{atom} as the vdW parameters for interaction with TIP3P water are unchanged [21]. Electric potentials and field components were computed using Equation 1 as well as Equation 2 with five different M-centers of TIP3P water; viz., (1) the water oxygen (M_O), (2) its geometric center (M_G), (3) its dipole center (M_μ), (4) its $H - H$ bisector (M_{HH}), and (5) the center ($M_{-\mu}$) obtained by reflection of M_μ about $H - H$ (see Figure 1A) [14]. The resulting electric potentials and field components were then compared with those obtained by solving Poisson equation with the dielectric boundary defined by R_{eff} (referred to as the 'two-sphere' continuum theory below) to assess the validity of the various schemes for summing potentials and fields. The $\langle \phi_\alpha^{elec} \rangle$ computed using Equation 1 and Equation 2 with various M-centers of TIP3P water were also used to compute electrostatic solvation free energies assuming linear solvent response.

2. Methodology

2.1. SIMULATION FORCEFIELD AND BOUNDARY CONDITIONS

To estimate R_{gmax} of the solute atoms, constant volume molecular dynamics (MD) simulations [17] of the model Na^{+q}–Cs^{-q} molecules in TIP3P water [23] were performed using the CHARMM version 27 program [25] at a mean temperature of 300 K. The simulations employed the minimum image convention and an atom-based *force*-switching function [26] which smoothly switches the nonbonded forces at 10 Å to zero at 11.7 Å. The nonbond pair list was updated every ten steps and the nonbond cut-off for the updates was set at 12.8 Å, i.e., half the length of the cubic simulation box. To verify the treatment of the long-range Coulombic forces in these 'spherical cut-off' simulations, simulation of Na^+–Cs^- was also carried out using the rectangular image charge (RIC) method without cut-offs [27]. The RIC method incorporates the effects of infinite solvent by using rectangular coordinates to solve for the potential in a dielectric cavity immersed in another dielectric material (see Figure 2). The calculations of the forces and energies using the RIC method are given in the Appendix.

2.2. SIMULATION PROTOCOL

The solute was fixed at the center of a cubic box of length 25.6 Å containing 560 previously equilibrated water molecules at a density of 1 g cc^{-1}. A water molecule was found to overlap with the solute atoms and was removed so the final system contained 559 TIP3P water molecules and the diatomic solute. The simulations employed the leapfrog Verlet algorithm with a time step of 2 fs. Each system was equilibrated for 20 ps and subjected to 100 ps of production dynamics, from which Na and Cs rdfs were computed. Solvation radii, R_{gmax}, were computed from

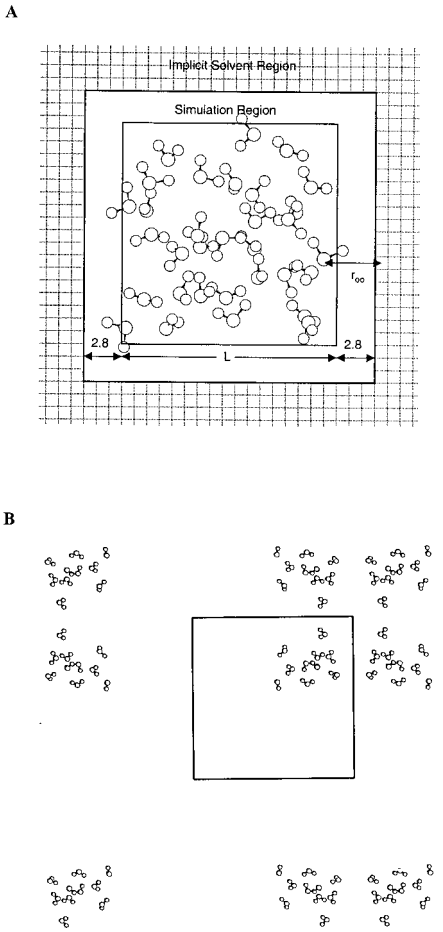

Figure 2. (a) A schematic representation of the simulation system in the rectangular image charge method. Water molecules in the simulation region cannot enter the implicit solvent region (hatched). The distance between the edge of the box (light solid) and the implicit solvent boundary (bold solid) is 2.8 Å, the distance to the first peak position of the water oxygen-water oxygen rdf. The boundary force on a water oxygen in the simulation region was calculated by summing its vdW interactions with water oxygen atoms in the implicit solvent region. (b) A two dimensional illustration of a 23.6 Å box containing 10 water molecules and their image charges.

the first peak position of the Na^{+q}-oxygen and Cs^{-q}-hydrogen rdfs, and used in Equation 3 to compute R_{eff}, which in turn were employed to define the dielectric boundary in finite-difference Poisson calculations (see below). Distance-dependent electrostatic potentials $\phi_\alpha^{elec}(R)$ were computed using the rdfs in Equation 1 as well as using Equation 2 with the M-center chosen as M_O, M_G, M_μ, M_{HH} and $M_{-\mu}$ (see Introduction).

2.3. NUMERICAL SOLUTION TO POISSON EQUATION

The electrostatic potential at a solute site due to a continuum solvent medium was obtained by solving the Poisson equation:

$$\nabla \cdot [\varepsilon(\mathbf{r})\nabla\phi(\mathbf{r})] + 4\pi\rho(\mathbf{r}) = 0 \tag{4}$$

where $\varepsilon(\mathbf{r})$ is a position-dependent dielectric constant and $\rho(\mathbf{r})$ is the charge density. Equation 4 was solved using finite difference methods with the Delphi program [28, 29]. A 65 Å × 65 Å × 65 Å grid and a percentage grid fill of 80% was employed. In conventional Delphi calculations a sphere of the same size as a water molecule is rolled over the solute surface, defined by the atomic coordinates and vdW radii of the solute atoms, to determine the low-dielectric solvent-inaccessible region. Such a procedure is not needed here since the definition of the effective Born radii R_{eff} in Equation 3 incorporates the solvent accessibility [22]. Hence, the solute cavity was defined by R_{eff}, with R_{gmax} of Na^{+q} (Cs^{-q}) equal to 2.38 (2.15), 2.45 (2.25), 2.58 (2.40), 2.70 (2.68) and 3.05 (2.88) Å for q = 1.0, 0.7, 0.5, 0.3 and 0.1e, respectively. (Note that the effective Born radius increases with decreasing charge on the solute atom). The error in R_{eff} is estimated to be less than ±0.03 Å, but it may be larger for $Na^{+0.1}$–$Cs^{-0.1}$ as its first solvation shell is less structured resulting in larger uncertainties in the R_{gmax} values of $Na^{+0.1}$ and $Cs^{-0.1}$. The dielectric constant inside the solute cavity (ε_{in}) was set to 1, while that outside (ε_{out}) was set to 80, the dielectric constant of bulk water.

3. Results

3.1. COMPARISON OF RESULTS FROM RECTANGULAR IMAGE CHARGE AND PERIODIC BOUNDARY SIMULATIONS

Figure 3 shows the distance dependence of the electrostatic potentials at Na^+ and Cs^- computed using the minimum image convention with spherical cut-offs (grey curves) and the RIC method with no cut-offs (black curves). Note that the RIC method includes the effects of infinite solvent, and has *no* periodicity-induced artifacts of periodic boundary with Ewald summation. The solid and dashed lines correspond to potentials based on q-summation and M_μ-summation, respectively. Figure 3 shows that the different treatments of the long-range Coulombic forces yield similar behavior of the potential values as a function of distance from the solute site, especially those based on M_μ-summation. This indicates that the long-range forces are adequately treated in the minimum image convention with spherical cut-offs presumably due to the dipolar nature of the solute considered here. Simulations using the RIC method for Na^{+q}–Cs^{-q} solutes of lower polarity ($q < 1e$) were not performed since long-range effects are expected to be even smaller compared to those for q = 1e. Consequently, the results below correspond to those from simulations using the minimum image convention and spherical cut-offs.

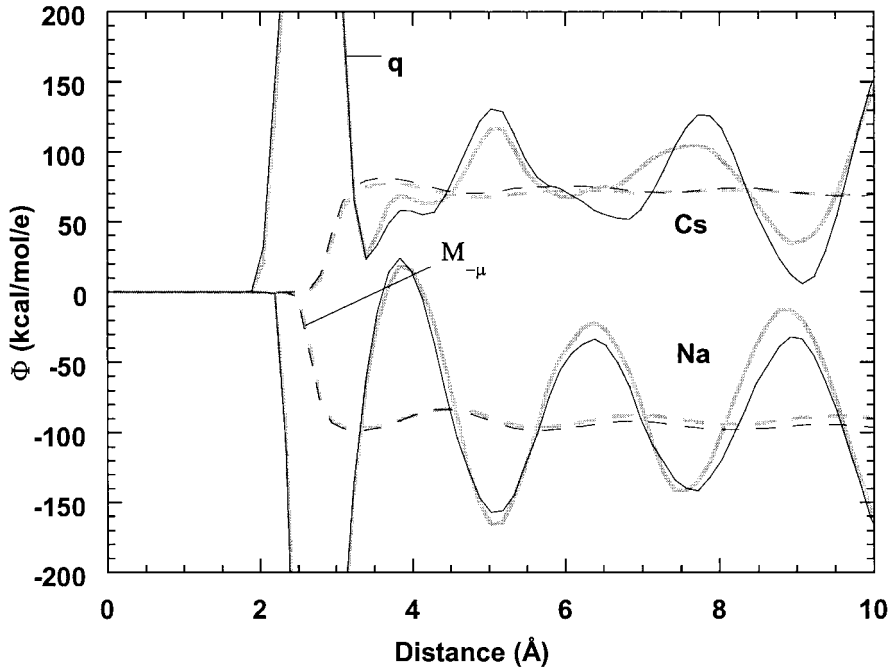

Figure 3. Comparison of q-summed (solid line) and M_μ-summed (dashed line) potentials obtained using the minimum image convention with spherical cut-offs (grey curves) and the rectangular image charge method with no cut-offs (black curves).

3.2. ELECTRIC POTENTIALS AND FIELD COMPONENTS AS A FUNCTION OF DISTANCE FROM THE SOLUTE SITE

Na^+ and Cs^-. Figure 4 shows the distance dependence of the electrostatic potentials and x-field components at Na^+ and Cs^- computed using various summation schemes. The results are shown up to only 10 Å since the nonbond cut-off is set at $\sim$ 12 Å (see Methods). The q-summed electric potentials (solid grey curves in Figure 4a) exhibit significant oscillations that persist even beyond 10 Å, indicating that splitting of the water charges at the cut-off sphere induces large contributions to the potential at Na^+ and Cs^-. In contrast to the q-summation results the M-summed electric potentials exhibit only slight oscillations after the second solvation shell ($\geq$ 7 Å), indicating that water molecules beyond the second shell are nearly randomly oriented with respect to the solute atom and thus contribute relatively little to the potential at Na^+ and Cs^- (Figure 4a). However, the M-summed electric potentials converge to different values depending on the molecular center. The magnitude of the potential at Na^+ and Cs^- is maximum using M_O and $M_{-\mu}$-summation, respectively, as water molecules orient with their oxygen pointing to Na^+ and their hydrogen pointing to Cs^-. Unlike the behavior of the M-summed potentials in Figure 4a, the M-summed electric x-field components merge after

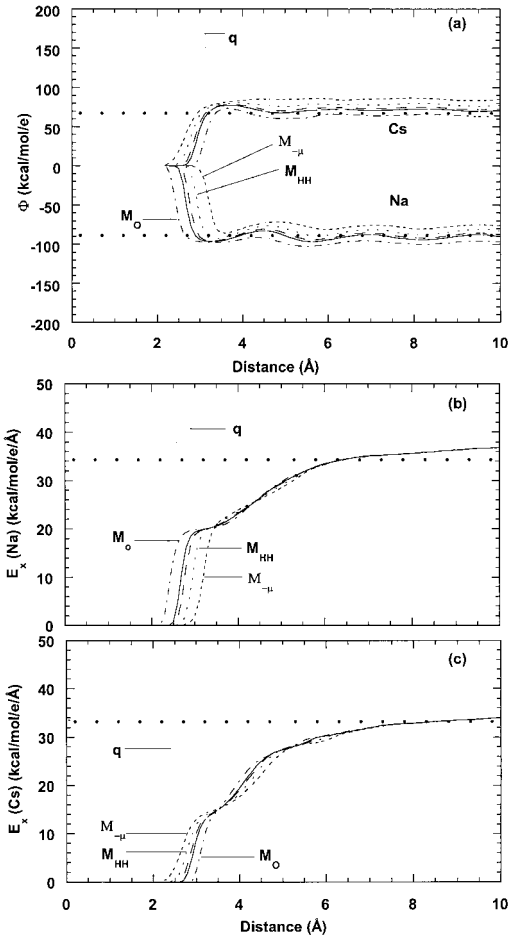

Figure 4. The fluctuations in the solvent-induced electrostatic potentials at Na^{+q} and Cs^{-q} (a) as well as the x-component of the electrostatic fields at Na^{+q} (b) and Cs^{-q} (c) as a function of the distance from the center of the solute atom for a charge state $q = 1e$. Note that the y- and z-field components in the simulations are nonzero (but very close to zero) due to distinct packing interactions of the solvent around the solute [10]. The horizontal dark dots are the theory results (i.e., $r = \infty$ values) obtained by solving Poisson equation using R_{eff} (Equation 3) to define the dielectric boundary. The solid grey curves are the q-summation results. The dash-dot, solid black, long-dash, short-dash, and dashed curves represent M-summations results based on M_O, M_μ, M_G, M_{HH}, and $M_{-\mu}$ centers, respectively.

7 Å and yield common values of 37 and 34 kcal mol^{-1} e^{-1} Å for Na^+ and Cs^-, respectively, at 10 Å(Figures 4b and 4c). This implies that the electric field and force components are not sensitive to the choice of the molecular center as long as the cut-off distance is greater than 7 Å. The M-summation results for the dipolar center (solid black curves) and geometric center (long-dash curves) of TIP3P water are similar as the two centers are only 0.1 Å apart.

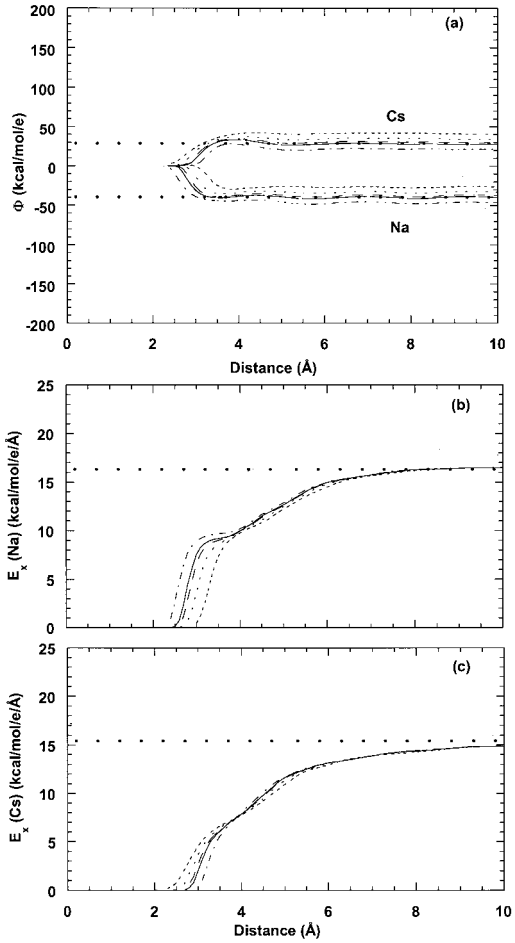

Figure 5. As in Figure 4 for a charge state $q = 0.5e$.

$Na^{+0.5}$ and $Cs^{-0.5}$. The trends in the electrostatic potentials and x-field components for $Na^{+0.5}$–$Cs^{-0.5}$ (Figures 5a-5c) are similar to those found for Na^{+}–Cs^{-} (Figures 4a-4c), except that the oscillations in the q-summed quantities for $Na^{+0.5}$ and $Cs^{-0.5}$ are milder than those observed for Na^{+} and Cs^{-} due to the weaker fields from the solute. For typical cut-off values of 8 to 12 Å employed in most simulations, the M-summed potentials converge faster with increasing cut-off distance than the q-summed ones, but the converged potentials depend on the choice of the M-center, whereas the electric field and force components do *not*. As for Na^{+}–Cs^{-}, the potential contribution from the first solvation shell is most negative (least positive) using M_O-summation and least negative (most positive) using $M_{-\mu}$-summation. Furthermore, the magnitude of the electrostatic potential or x-field component at 10 Å for the positively charged Na site is larger than the respective value for the negatively charged Cs site due mainly to the non-random orientations

of water molecules in the first shell. The features and trends in the electrostatic potentials and field components as a function of distance from the solute site for the other charge states of Na^{+q}–Cs^{-q} (q = 0.1, 0.3 and 0.7e) are similar to those depicted in Figures 4 and 5.

3.3. COMPARISON BETWEEN SIMULATION AND THEORY

Electric field components: Figures 4 and 5 also show the electrostatic potentials and x-field components at the solute sites obtained from finite difference solutions to the Poisson equation with the dielectric boundary defined by R_{eff} in Equation 3 (dark-dotted horizontal lines). The M-summed x-field components at the solute sites, which converge to the same value *independent* of the molecular center, are close to the corresponding values obtained from the 'two-sphere' continuum theory. For example, the converged M-summed x-field components (16.5 ± 0.7 kcal mol^{-1} e^{-1} Å for $Na^{+0.5}$ and 14.8 ± 0.5 kcal mol^{-1} e^{-1} Å for $Cs^{-0.5}$) are in excellent agreement with the theoretical values (16.3 kcal mol^{-1} e^{-1} Å for $Na^{+0.5}$ and 15.4 kcal mol^{-1} e^{-1} Å for $Cs^{-0.5}$). In contrast the magnitudes of the q-summed electric x-field components as well as q-summed potentials at 10 Å are significantly larger than the respective 'two-sphere' continuum theory results. These findings suggest that q-summation using typical cut-off distances of 8–10 Å yields erroneous electric x-field components and potentials. As rationalized in previous works [13, 18] this is because q-summation violates intramolecular site-site correlation and the self-consistency of statistical sampling of solvent configurations contributing to the average electrostatic potential.

Electrostatic potentials: Figures 4a and 5a show that at 10 Å the M_μ and M_G-summed potentials are remarkably close to the corresponding values derived from the 'two-sphere' continuum theory. For example, the M_μ and M_G-summed potentials at 10 Å for $Na^{+0.5}$ (-40.0 ± 1.5 and -38.0 ± 1.4 kcal mol^{-1} e^{-1}) and $Cs^{-0.5}$ (27.7 ± 1.6 and 29.9 ± 1.2 kcal mol^{-1} e^{-1}) are in accordance with the theoretical values (-38.0 and 28.7 kcal mol^{-1} e^{-1} for $Na^{+0.5}$ and $Cs^{-0.5}$, respectively). However, potentials summed over other molecular centers like M_{HH}, M_O and $M_{-\mu}$ deviate significantly from both theory and the M_μ or M_G-summed results. These trends also apply for other charged states, as illustrated in Figures 6a and 6b, which depict the potentials at Na^{+q} and Cs^{-q}, respectively, for q ranging from 1.0 to 0.1e. The converged values of the electrostatic potentials computed using M_μ-summation (solid black curves) and M_G-summation (long-dash curves) match those obtained from the 'two-sphere' continuum theory (filled circles), although the agreement for M_μ-summation is overall better than that for M_G-summation especially at higher solute polarity. In contrast to the M_μ and M_G-summed results, electrostatic potentials based on alternative M-centers or q-summation deviate from the respective theory values. In particular, the deviations of the q-summed electric potentials (solid grey curves) at Na^{+q} and Cs^{-q} magnify dramatically as the solute polarity is increased.

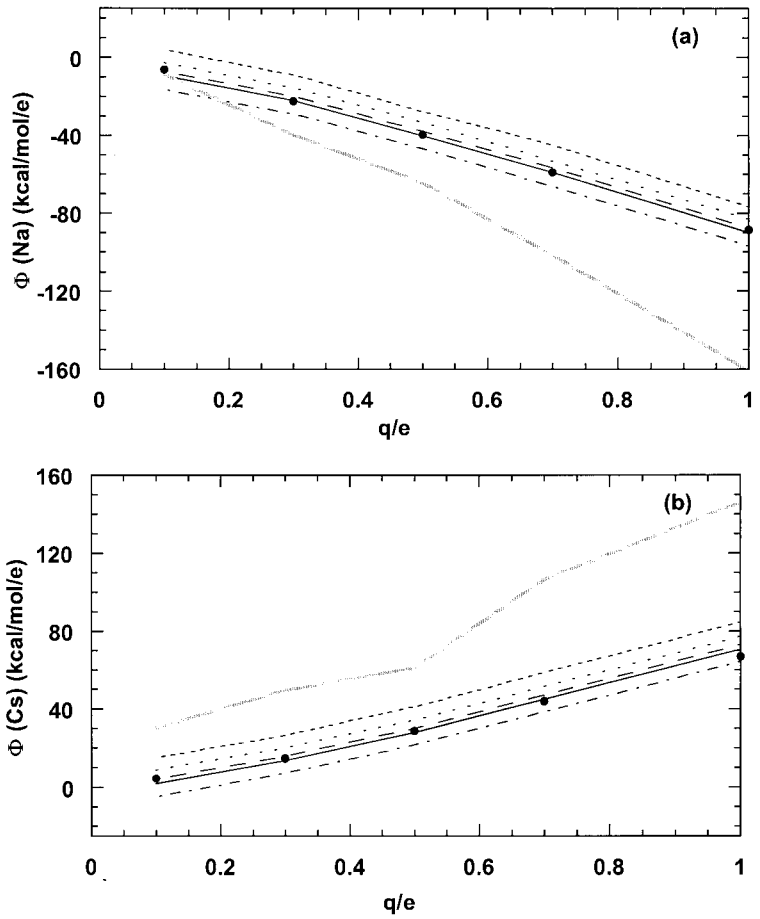

Figure 6. Electrostatic potentials at Na^{+q} (a) and Cs^{-q} (b) as a function of solute charge q. The symbols have the same meaning as in Figure 4.

3.4. APPLICATIONS OF THE ELECTROSTATIC POTENTIAL: THE VALIDITY OF THE LINEAR RESPONSE APPROXIMATION

An important application of the electrostatic potential is in estimating the electrostatic contribution to the solvation free energy assuming linear response of the solvent [30, 31]; i.e.,

$$\Delta G^{LR} = \frac{1}{2} \sum_{\alpha} q_{\alpha} \langle \phi_{\alpha}^{elec} \rangle \tag{5}$$

In Equation 5, $\langle \phi_{\alpha}^{elec} \rangle$ is the ensemble average of the solvent electrostatic potential from an all-atom molecular dynamics simulation. Previous work had tested the linear response approximation using M_O-summation of the potential [3]. Here, we

Table I. Comparison of electrostatic solvation free energies of Na^{+q}–Cs^{-q} obtained from the 'two-sphere' continuum theory and the linear response formula with those from free energy simulations

	$-\Delta G^{a}$	$-\Delta G^{b}$	$-\Delta G^{c}$				
$\|q\|/e$			q	M_O	M_μ	M_{HH}	$M_{-\mu}$
0.1	0.4 ± 0.1	0.5	0.6	0.6	0.6	0.6	0.6
0.3	5.0 ± 0.3	5.5	12.0	5.4	5.3	5.3	5.3
0.5	15.9 ± 0.3	16.8	31.4	17.0	17.0	16.9	16.9
0.7	34.3 ± 0.4	35.6	72.6	36.8	36.3	36.2	36.2
1.0	76.7 ± 0.4	76.6	155.0	80.9	80.5	80.4	80.8

[a] From free energy perturbation simulation from Reference [22]. [b] Electrostatic solvation free energies derived by solving Poisson equation using R_{eff} (Equation 3) to define the dielectric boundary. [c] Free energies computed using the linear response approximation (Equation 5) and q, M_O, M_μ, M_{HH}, or $M_{-\mu}$-summation of the electrostatic potential (see text).

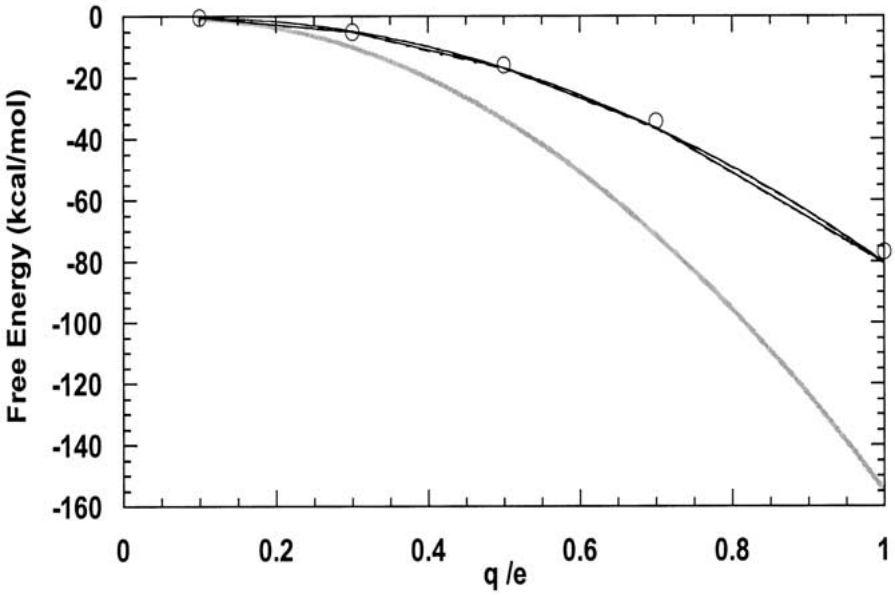

Figure 7. Free energies as a function of solute charge q. The symbols have the same meaning as in Figure 4, but they correspond to free energies computed using the linear response formula (Equation 5). The open circles correspond to free energy simulation results.

test the validity of linear solvent response by computing $\langle \phi_\alpha^{elec} \rangle$ using Equation 1 and Equation 2 with various M-centers of TIP3P water. Comparison of the electrostatic solvation free energies of Na^{+q}–Cs^{-q} computed using Equation 5 with those obtained from free energy perturbation simulations in our previous work [22] (Table I and Figure 7) shows that q-summation of the potentials yields ΔG^{LR} that deviate significantly from the respective simulation free energies. In contrast, M-summation yields ΔG^{LR} in close agreement with the corresponding simulation values (Table I and Figure 7). Furthermore, the ΔG^{LR} values are *not* sensitive to the choice of the molecular center unlike the electrostatic potentials.

Note that when $|q| = 0.1$e, both q- and M-summation of the potentials yield the same ΔG^{LR}, even though $\langle \phi_\alpha^{elec} \rangle$ computed using q-summation differs from that computed using M-summation. This is consistent with the finding that periodic boundary and Ewald summation with vacuum ($\varepsilon = 1$) or tin-foil ($\varepsilon = \infty$) boundary conditions as well as spherical boundary with a spherical cut-off all yield the same polarization free energy for charging a probe water molecule (–8.4 kcal mol^{-1}), but different solvent-induced electrostatic potentials [18].

The ΔG^{LR} values obtained using M-summation of the potentials slightly overestimate the respective values from free energy perturbation simulations (Table I). Agreement between the linear response free energies and the corresponding free energy perturbation results could be achieved if a factor slightly lower than 0.5 is employed in Equation 5; i.e., 0.48, 0.47 and 0.45 for q = 1.0, 0.7 and 0.5e, respectively. The deviation from 0.5, which indicates deviations of linear solvent response, has also been found for similar dipolar solutes in previous work [13]. The results in Table I suggest that accurate electrostatic free energy differences between two similarly shaped molecules in water may be obtained from M-summed electrostatic potentials (using Equation 5) instead of the more compute-intensive free energy simulations once an appropriate factor is identified for such systems.

4. Discussion

The results in the previous section (Figures 4–6) indicate the existence of a molecular center of TIP3P water, viz., its dipole center (M_μ), which, when used in Equation 2, gives electrostatic potentials at Na^{+q} and Cs^{-q} that consistently match those derived from the 'two-sphere' continuum theory for solute charges ranging from 1 to 0.1e (corresponding to decreasing solute-solvent electrostatic interactions). Åqvist and Hansson [3] also found the dipole center of water to be the 'best center' in M-summation because the potential created by the surface layer around the cut-off is minimized with this choice of the molecular center in M-summation.

4.1. THE PHYSICAL BASIS FOR THE DIPOLAR CENTER OF TIP3P WATER

The contributors to the total electric potential and field component at a solute site are mainly water molecules forming the first solvation shell and to a lesser extent

those in the second shell. For q = 1e (Figure 4), the M_μ-summed potentials level out after $\sim$ 7 Å, corresponding roughly to the radius of the second solvation shell. Similar trends are observed for q = 0.5e (Figure 5). Thus, the main factor governing the sign and the magnitude of the electric potentials and fields is the specific orientation of water molecules in the first and second solvation shells. This is supported by the finding that the contribution to the total solvation energy from the first (0–4 Å) shell around a chloride ion from a MD trajectory (–87 kcal mol^{-1}) differs from that obtained by replacing water molecules in the simulation with point dipoles of the same dipole moment as TIP3P or SPC water (–67 kcal mol^{-1}) [32]. However, beyond the first shell, water molecules appear as dipoles to the solute as the solvation energy contributions from the second (4–6 Å) shell and beyond were similar for the all-atom and point dipole models [32]. Likewise, replacing water molecules far from an uncharged solute by *two*-point dipoles has been found to yield potentials that are in accord with those from an all-atom model [13]. This shows that a point dipole or *two*-point linear dipole approximation for water molecules outside the first or second solvation shells of a charged or uncharged solute could adequately represent water orientations, and thus quadrupole terms can be neglected at a sufficiently large cut-off distance.

The physical origin of the dipolar center of three-site water models for computing potentials and fields can also be rationalized by considering the interaction of a point dipole solvent of dipole moment μ with an ion of charge q in a continuum solvent characterized by a dielectric constant ε [32]. The average solvation energy of the ion due to the solvation shell between R_1 and R_2 from the ion is related to the orientational probability of the point dipole $P(\cos\theta; r)$ (θ is the orientational angle between the dipole vector and the internuclear ion-water dipole vector) at a distance r via the following equation:

$$\begin{aligned}\langle U(R_1; R_2)\rangle &= -4\pi\rho \int_{R_1}^{R_2} dr \int_{-1}^{+1} d\cos(\theta)\mu q\cos(\theta) g(r) P(\cos\theta; r) \\ &= -4\pi\rho\mu q \int_{R_1}^{R_2} dr g(r)\langle\cos\theta\rangle_r\end{aligned} \tag{6}$$

In Equation 6, ρ is the dipole density and $g(r)$ is the ion-dipole rdf and the angular brackets indicate an ensemble average. The probability $P(\cos\theta, r)$ is given by [32]:

$$P(\cos\theta; r) = \frac{\exp[\beta\mu E(r)\cos\theta]}{2\sinh[\beta\mu E(r)]/[\beta\mu E(r)]} \tag{7a}$$

or

$$\langle\cos\theta\rangle_r = \coth[\beta\mu E(r)] - 1/[\beta\mu E(r)] \tag{7b}$$

where $E(r) = q/\varepsilon r^2$ is the field at the dipole due to the ion. The orientational probabilities from Equation 7 (which treats water as a point dipole) have been shown

to be similar to those obtained from simulations of a chloride ion in TIP3P/SPC water for distances greater than 7 Å [32]. This implies that the electrostatic contributions to the solvation energy (Equation 6), and thus the potential, from 3-site water molecules at a distance greater than 7 Å from the solute are from solvent dipoles. Most simulations employ a potential cut-off between 8 and 12 Å, which is sufficiently far away from the ion and the first or second solvation shell.

4.2. EXTENSION TO COMPLEX MOLECULAR SYSTEMS

The present findings apply to a solute in a rigid 3-site model of water. The choice of a molecular center in a more complex classical mechanical or in a quantum mechanical description of the solvent (including non-aqueous solvents) requires further study. One way is to divide the solvent molecule into neutral groups and perform calibrations as in this study for TIP3P water to identify a suitable M-center. For polar macromolecules, an amino acid residue is generally divided into small neutral polar groups as in the CHARMM program [25]. Since the forces are not sensitive to the choice of the M-center (see Results), the outcome of MD calculations would be similar for any reasonable choice of the M-center for such groups since only the forces determine the MD trajectory.

5. Conclusions

Although the M-summed electrostatic potentials at Na^{+q} and Cs^{-q} (Equation 2) depend on the choice of the solvent molecular center (Figures 4 and 5), they yield linear response free energies, ΔG^{LR} (Equation 5), of Na^{+q}–Cs^{-q} that are *not* sensitive to the M-center (see Table I). Furthermore, the M-summed electrostatic potentials yield ΔG^{LR} of the Na^{+q}–Cs^{-q} solutes for q varying from 1.0 to 0.1e in close agreement with the respective values derived from free energy perturbation simulations, whereas the q-summed potentials yield ΔG^{LR} that deviate significantly from free energy simulations (see Figure 7 and Table I). The observed close agreement between the linear response free energies based on M-summation and the corresponding free energy perturbation results also suggests that the linear response formula, Equation 5, is valid.

It is noteworthy that the 'two-sphere' continuum theory predicts electrostatic solvation free energies in excellent agreement with respective values derived from free energy simulations in the presence of explicit water molecules (see Table I). In particular, it reproduces the non-quadratic charge dependence of the solvation free energies (Table I) as well as the non-linear charge dependence of the M_μ and M_G summed potentials at Na^{+q} and Cs^{-q} (Figure 6).

M_μ-summation yields not only electrostatic solvation free energies of Na^{+q}–Cs^{-q}, but also electrostatic potentials and field components at Na^{+q} and Cs^{-q} that consistently match those derived from the 'two-sphere' continuum theory for solute charges ranging from 1 to 0.1e (corresponding to decreasing solute-solvent

electrostatic interactions, see Figure 6). Thus there appears to be a convenient molecular center for 3-site water models (like TIP3P and SPC), namely, the dipole center of water, in computing electrostatic potentials and field components using M-summation. In contrast, q-summation using cut-offs that are ≤ 10 Å generally underestimates or overestimates the magnitude of the potentials and field components at Na^{+q} and Cs^{-q} relative to the theoretical values as well as ΔG^{LR} of Na^{+q}–Cs^{-q} relative to the respective free energies from free energy perturbation simulations (Figures 4 to 7).

Appendix

RECTANGULAR IMAGE CHARGE METHOD

Consider N point charges, $Q_1(R_1)$, $Q_2(R_2) \ldots Q_N(R_N)$, in a dielectric ε_a, bounded by a cubic box of length L, which separates the medium from another dielectric ε_w (see Figure 2). In the image charge method, the electric potential at a distance $\mathbf{R}_i = \{x_i, y_i, z_i\}$ in ε_a can be evaluated by placing image charges,

$$Q_{j,l,m,n} = Q_j \left(\frac{\varepsilon_a - \varepsilon_w}{\varepsilon_a + \varepsilon_w} \right)^{|l|+|m|+|n|} \tag{8}$$

at:

$$\mathbf{R}_{j,l,m,n} = \{x_{j,l}, y_{j,m}, z_{j,n}\} = \{(-1)^l x_j + la, (-1)^m y_j + mb, (-1)^n z_j + nc\}. \tag{9}$$

The electric potential at a distance $\mathbf{R}_i$ is then given by:

$$\phi(\mathbf{R}_i) = \sum_{j=1}^{N} \frac{Q_j}{4\pi\varepsilon_a |\mathbf{R}_i - \mathbf{R}_j|} + \sum_{j=1}^{n} \sum_{\substack{l,m,n=-\infty \\ l^2+m^2+n^2 \neq 0}}^{\infty} \frac{Q_{j,l,m,n}}{4\pi\varepsilon_a |\mathbf{R}_i - \mathbf{R}_{j,l,m,n}|} \tag{10}$$

and the total electrostatic energy U in the box can be evaluated by:

$$U = \sum_{i=1}^{N} \sum_{j=i+1}^{N} \frac{Q_i Q_j}{4\pi\varepsilon_a |\mathbf{R}_i - \mathbf{R}_j|} + \frac{1}{2} \sum_{i,j=1}^{N} \sum_{\substack{l,m,n=-\infty \\ l^2+m^2+n^2 \neq 0}}^{\infty} \frac{Q_i Q_{j,l,m,n}}{4\pi\varepsilon_a |\mathbf{R}_i - \mathbf{R}_{j,l,m,n}|}. \tag{11}$$

The first term in Equation 12 represents the direct electrostatic interactions between the real charges in the simulation region, while the second term represents the interactions between each charge and all image charges. The force at atom i is given by:

$$\mathbf{F}_i(\mathbf{R}) = \sum_{\substack{j=1 \\ j \neq i}}^{N} \frac{Q_i Q_j (\mathbf{R}_i - \mathbf{R}_j)}{4\pi\varepsilon_a |\mathbf{R}_i - \mathbf{R}_j|^3} + \sum_{j=1}^{n} \sum_{\substack{l,m,n=-\infty \\ l^2+m^2+n^2 \neq 0}}^{\infty} \frac{Q_i Q_{j,l,m,n} (\mathbf{R}_i - \mathbf{R}_{j,l,m,n})}{4\pi\varepsilon_a |\mathbf{R}_i - \mathbf{R}_{j,l,m,n}|^3}. \tag{12}$$

In computing the image charges using Equation 9 ε_a and ε_w were set equal to 1 and 80, respectively. As water molecules approach the implicit solvent boundary,

the second term in Equation 12 will go to infinity, hence vdW interactions between water oxygen atoms in the simulation and implicit solvent regions were included to prevent water molecules from approaching too close to the implicit solvent boundary. Thus, a water oxygen at position **r** in the simulation region (Figure 2) was subjected to a boundary force of the form:

$$F_w = 0.0 \qquad w \leq L/2 - 5 \tag{14a}$$

$$F_w = 0.05 \qquad L/2 - 5 < w \leq L/2 \tag{14b}$$

$$F_w = (w - L/2 - 2.8)^2 - 2.8^2 \qquad L/2 < w < L/2 + 2.8 \tag{14c}$$

In Equation 14, w denotes x, y or z and L is the length of the cubic box. The derivation of Equations 9–14 is given in Reference [27].

Acknowledgements

We thank Professor Martin Karplus for the CHARMM program. This work was supported by the National Science Council, Taiwan (NSC contract # 88-2113-M-001-072) and the National Center for High-Performance Computing, Taiwan.

References

1. Levy, R.M., Belhadj, M. and Kitchen, D.B.: Gaussian fluctuation formula for electrostatic free energy changes in solution, *J. Chem. Phys.* **95** (1991), 3627–3633.
2. Hummer, G., Pratt, L.R. and Garcia, A.E.: Free energy of ionic hydratrion, *J. Phys. Chem.* **100** (1996), 1206–1215.
3. Åqvist, J. and Hansson, T.: On the validity of electrostatic linear response in polar solvents, *J. Phys. Chem.* **100** (1996), 9512–9521.
4. Ashbaugh, H.S.: Convergence of molecular and macroscopic continuum descriptions of ion hydration, *J. Phys. Chem. B* **104** (2000), 7235–7238.
5. Yelle, R.B. and Ichiye, T.: Solvation free energy curves for electron transfer in aqueous solution: Theory and simulation, *J. Phys. Chem. B* **101** (1997), 4127–4135.
6. Lee, F.S., Chu, Z.-T., Bolger, M.B. and Warshel, A.: Calculations of antigen-antibody interactions: Microscopic and semi-microscopic evaluation of the free energies of binding of phosphorylcholine analogs to McPC603, *Prot. Engng.* **5** (1992), 215—228.
7. Åqvist, J., Medina, C. and Samuelson, J.-E.: A new method for predicting binding affinity in computer-aided drug design, *Prot. Engng.* **7** (1994), 385–391.
8. Carlson, H.A. and Jorgensen, W.L.: An extended linear response method for determining free energies of hydration, *J. Phys. Chem.* **99** (1995), 10667–10673.
9. Wilson, M.A., Pohorille, A. and Pratt, L.R.: Comment on 'Study on the liquid-vapor interface of water. I. Simulation results of thermodynamic properties and orientational structure', *J. Chem. Phys.* **90** (1989), 5211–5213.
10. Rick, S.W. and Berne, B.J.: The aqueous solvation of water: A comparison of continuum methods with molecular dynamics, *J. Am. Chem. Soc.* **116** (1994), 3949–3954.

11. Hummer, G., Pratt, L.R., Garcia, A.E., Berne, B.J. and Rick, S.W.: Electrostatic potentials and free energies of solvation of polar and charged molecules, *J. Phys. Chem. B* **101** (1997), 3017–3020.
12. Hansen, J.P. and McDonald, I.R.: *Theory of simple liquids*, Academic Press, 1986.
13. Åqvist, J. and Hansson, T.: Analysis of electrostatic potential truncation schemes in simulations of polar solvents, *J. Phys. Chem. B* **102** (1998), 3837–3840.
14. Ashbaugh, H.S., Sakane, S. and Wood, R.H.: Reply to comment on 'Electrostatic potentials and free energies of solvation of polar and charged molecules', *J. Phys. Chem. B* **102** (1998), 3844–3845.
15. Darden, T., Pearlman, D. and Pedersen, L.G.: Ionic charging free energies: Spherical versus periodic boundary conditions, *J. Chem. Phys.* **109** (1998), 10921–10935.
16. Hummer, G., Pratt, L.R., Garcia, A.E., Garde, S., Berne, B.J. and Rick, S.W.: Reply to comment on 'electrostatic potentials and free energies of solvation of polar and charged molecules', *J. Phys. Chem. B* **102** (1998), 3841–3843.
17. Allen, M.P. and Tildesley, D.J.: *Computer Simulation of Liquids*, Oxford University Press, NY, 1990.
18. Vorobjev, Y.N. and Hermans, J.: A critical analysis of methods of calculation of a potential in simulated polar liquids: Strong arguments in favor of 'molecule-based' summation and of vacuum boundary conditions in Ewald summation, *J. Phys. Chem. B* **103** (1999), 10234–10242.
19. Babu, C.S. and Lim, C.: Theory of ionic hydration: Insights from molecular dynamics simulations and experiment, *J. Phys. Chem. B* **103** (1999), 7958–7968.
20. Madhusoodanan, M. and Lim, C.: 2002, in preparation.
21. Babu, C.S. and Lim, C.: Solvation free energies of polar molecular solutes: Application of the two-sphere Born radius in continuum models of solvation, *J. Chem. Phys.* **114** (2001), 889–899.
22. Babu, C.S. and Lim, C.: Incorporating nonlinear solvent response in continuum dielectric models using a two-sphere description of the Born radius, *J. Phys. Chem.* **105** (2001), 5030–5036.
23. Jorgensen, W.L., Chandrasekhar, J., Madura, J.D., Impey, R.W. and Klein, M.L.: Comparison of simple potentials for simulating liquid water, *J. Chem. Phys.* **79** (1983), 926–923.
24. Åqvist, J.: Ion-water potentials derived from free energy perturbation simulations, *J. Phys. Chem.* **94** (1990), 8021–8024.
25. Brooks, B.R., Bruccoleri, R.E., Olafson, B.D., States, D.J., Swaminathan, S. and Karplus, M.: CHARMM: A program for macromolecular energy, minimization, and dynamics calculations, *J. Comp. Chem.* **4** (1983), 187–217.
26. Steinbach, P.J. and Brooks, B.R.: New spherical-cut-off methods for long-range forces in macromolecular simulation, *J. Comp. Chem.* **15** (1994), 667–683.
27. Yang, P.-K., Liaw, S.-H. and Lim, C.: Representing an infinite solvent system by a rectangular finite system using image charges, *J. Phys. Chem. B* (2002). in press.
28. Sharp, K.A. and Honig, B.: Electrostatic interactions in macromolecules: Theory and applications, *Ann. Rev. Biophys. Biophys. Chem.* **19** (1990), 310–332.
29. Nicholls, A. and Honig, B.: A rapid finite difference algorithm utilizing successive over-relaxation to solve the Poisson-Boltzmann equation, *J. Comp. Chem.* **12** (1991), 435–445.
30. Warshel, A. and Russell, S.T.: Calculation of electrostatic interactions in biological systems and in solution, *Quart. Rev. Biophys.* **17** (1984), 283–422.
31. Roux, B., Yu, H.-A. and Karplus, M.: Molecular basis for the Born model of ion solvation, *J. Phys. Chem.* **94** (1990), 4683–4688.
32. Hyun, J.-K., Babu, C.S. and Ichiye, T.: Apparent local dielectric response around ions in water: A method for its determination and its applications, *J. Phys. Chem.* **99** (1995), 5187–5195.